Characterization of metamorphic $In_xAl_{1-x}As/GaAs$ buffer layers using reciprocal space mapping

D. Lee, M. S. Park,[a] and Z. Tang
Department of Electrical Engineering, State University of New York at Buffalo, Buffalo, New York 14260

H. Luo and R. Beresford
Division of Engineering, Brown University, Box D, Providence, Rhode Island 02912

C. R. Wie[b]
Department of Electrical Engineering, State University of New York at Buffalo, Buffalo, New York 14260

(Received 5 October 2006; accepted 18 January 2007; published online 23 March 2007)

The depth profiles of metamorphic $In_xAl_{1-x}As$ $(0.05<x<1)$ buffer layers grown on GaAs substrates were characterized using the x-ray reciprocal space mapping. Three types of metamorphic samples were investigated and compared: step grade, single-slope linear grade, and dual-slope linear grade. The lattice mismatch, residual strain, crystallographic tilt, tilt azimuth, and the full width at half maximum were obtained from the reciprocal space maps. The tilt angle of linearly graded buffer layers stayed low at low In compositions until In≈60%, at which composition the tilt angle increased abruptly. All linear-grade samples had an untilted relaxed structure in the low In region (below 60% In) and a tilted structure in the upper, high In region (above 60% In). The average lattice mismatch between the untilted relaxed structure and the tilted structure determines the tilt angle. The tilt angle of the step-graded layers increased at a near-linear rate as the In composition was increased. The tilt azimuth was intermediate between the ⟨100⟩ and ⟨110⟩ in-plane directions. The x-ray full width at half maximum generally increased with the In composition, but tended lower toward surface. We suggest a possible design strategy for the linear-grade metamorphic buffer layer based on our result. © *2007 American Institute of Physics*. [DOI: 10.1063/1.2711815]

I. INTRODUCTION

InAs-based structures are of great interest for high speed and low power applications due to its high electron mobility (33 000 $cm^2/V\,s$) and a small band gap energy (0.36 eV). However, the cost to manufacture the InAs substrate is high and also the reproducibility is poor. Therefore, it is better to grow InAs layers on less costly substrates such as GaAs. Since the lattice mismatch between InAs and GaAs is about 7.2%, we have to use metamorphic graded buffer layers to confine misfit dislocations which are nucleated by the lattice constant discrepancy. This is the main reason why epitaxial growth of metamorphic materials is often used as a buffer layer between the active layer and the substrate. A mismatch of 1% in the lattice parameters can result in a high density $(>10^9\ cm^{-2})$ of device-degrading dislocations.[1] An ideal buffer layer must be chemically compatible with the growth conditions of the active layers, completely relaxed, and have a smooth surface.[2] Metamorphic buffer layers, which change the composition gradually along the layer thickness, allow an arbitrary combination of active semiconductor structures to be formed on a substrate having a different lattice constant. These buffers are essential to accommodating the lattice mismatch between the active layers and the substrate in a controllable way, generating a substrate with a desired lattice constant, and moderating the dislocation densities.[3] Various buffer layers with compositional gradients have been developed with growth of InGaAs,[4–7] InAlAs,[6,8] or InAlGaAs (Refs. 9 and 10) materials on GaAs substrate and SiGe (Ref. 11) on Ge substrate. Buffer layers containing Al were preferable because they ensure good insulating properties. Many investigations were done on different samples, structures, and growth scheme.[3–12] However, there are few studies about different growth schemes with samples having a similar composition.

The aim of this work is to investigate the structural properties and relaxation behaviors of the metamorphic buffers as a function of layer composition and thus we produce a depth profile. The high resolution x-ray diffraction technique was applied to various InAlAs samples having different growth schemes. Reciprocal space maps (RSMs) describe well the tilt status, the relaxation status, and the composition of the metamorphic structures, often more effectively than the x-ray rocking curves. Triple-crystal diffraction allowed the determination of contributions to the RSM data from strain, tilt, and mosaic spread. The depth profiles of FWHM and tilt angle, as they corresponded to the composition, were extracted from the RSM analysis procedure. We discuss our depth profile data of tilt angles in view of the literature on the tilted growth of lattice-mismatched heterostructures such as α-Si_3N_4/Si,[13] Cu and compound films on GaAs,[14] and hcp rare earth metal layers on bcc transition metal substrates.[15]

[a]Present address: Advanced Technology Team, Samsung Electronics Co., Ltd, No. 200 Myungam-Rhi, Tangjeong-Myeon, Asan-City, Chungcheongnam-do 36-841, Korea.
[b]Author to whom correspondence should be addressed; electronic mail: wie@buffalo.edu

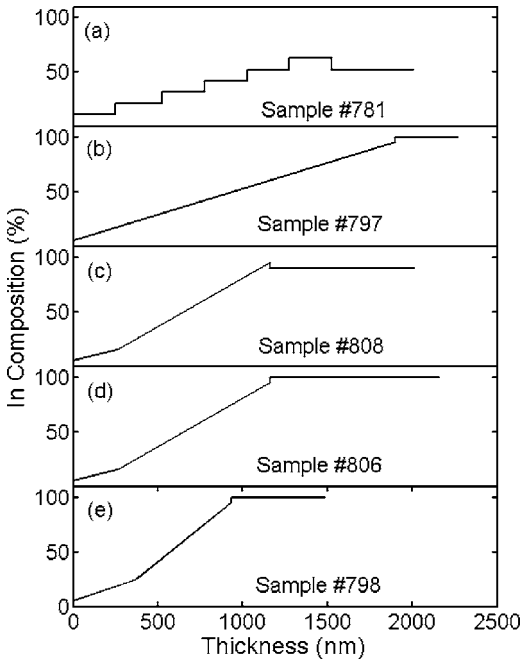

FIG. 1. Grading profiles for the $In_xAl_{1-x}As$ metamorphic buffer layers grown on a (001) GaAs substrate: (a) step-grade (781), (b) single-slope linear grade (797), (c) dual-slope linear grade with inverse step top layer (808), (d) dual-slope linear grade with step-up top layer (806), and (e) dual-slope linear grade with steeper grading (798).

II. EXPERIMENTS AND RESULTS

The growth of metamorphic layers was performed in an EPI-930 molecular beam epitaxy (MBE) system. The substrates are a 2 in. diameter semi-insulating GaAs wafer with (001) orientation. The wafers were thermally cleaned at about 590 °C with an As_4 beam-equivalent pressure of 1.5×10^{-5} Torr until the native oxide was desorbed and a clear As-stable (2×4) diffraction pattern was confirmed. Prior to the metamorphic layer growth, a GaAs buffer layer of 250 nm was grown at 580 °C. The nominal growth rate for all samples was 0.28 nm s^{-1}.

Figure 1 shows the growth scheme of the three different types of $In_xAl_{1-x}As$ metamorphic buffers we investigated. They are the step-grading [Fig. 1(a)] and two types of linear-grading, single slope [Fig. 1(b)] and dual slope [Figs. 1(c)–1(e)]. In the layer structure of the step-graded sample [781, Fig. 1(a)], the In content increased at about 10% per step for the first six layers and the top layer is an inverse step layer with less In than the previous layer. These parameters were chosen to lattice match the top $In_{0.52}Al_{0.48}As$ layer with InP. The second sample [797, Fig. 1(b)] was a single-slope linearly graded buffer, which consisted of a 2000 nm metamorphic $In_xAl_{1-x}As$ layer in which the content of In increases from 5% to 95% with a constant slope, capped by a 360 nm InAs top layer. The third sample type was a linearly graded buffer layer with a dual slope in the In composition grade. There were three samples in this type. The first had a buffer with a first grading slope of 38.5% In/μm for the In content ranging from 5% to 15% and a second grading slope of 88.9% In/μm for the In content increasing from 15% to 95% followed by a 850 nm top layer of inverse step with 90% In content [808, Fig. 1(c)]. Another linearly graded dual-slope sample [806, Fig. 1(d)] was identical to the first one (808) except that it had an InAs top layer of 1000 nm in thickness. The third sample [798, Fig. 1(e)] had a buffer with a steeper grading slope of 53.3% In/μm for the In content changing from 5% to 25%, followed by a buffer with grading of 125% In/μm and In content varying from 25% to 95%. The top layer was 540 nm of InAs.

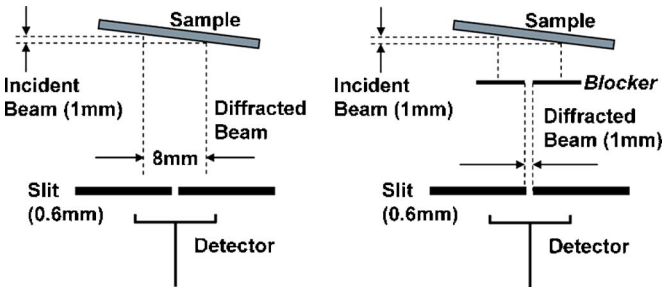

FIG. 2. RSM measurement setup for GaAs (224). In all of our 224 RSM measurements, a 1-mm-wide blocker was placed between the sample and the 0.6 mm detector slit.

A Huber 512.5 four-circle diffractometer was used for high-resolution triple-axes reciprocal space maps. A Bartels-type four-bounce monochromator, Ge (220) reflection, was used in the incident beam. The sample was mounted on a four-axis sample holder, in which each axis was controlled by a stepper motor. The stepper precision was about 0.0025°. The analyzer crystal was not necessary in this study because the x-ray diffraction peaks were rather broad. Acting as a low-resolution analyzer was a 0.6-mm-wide slit positioned before the detector, which set the detector aperture at about 295 arc sec. The use of a slit instead of an analyzer crystal allowed a higher intensity at the detector due primarily to the increased acceptance angle at the detector. Reciprocal space maps were obtained by performing a series of 2θ scans of the detector while incrementing the sample angular position ω between the 2θ scans. Since a symmetrical diffraction is only sensitive to the lattice spacing perpendicular to the sample surface, an asymmetrical diffraction is needed for information about the in-plane lattice spacing. Therefore, both symmetric (004) and asymmetric (224) RSM data were measured at four different azimuthal angles of the sample.

We used the low angle of incidence (7°) for an increased diffraction intensity. The low angle incidence data of GaAs(224) RSM show an elongation along the ⟨110⟩ directions since the reflected beam size is about 8 mm, resulting in a poor 2θ resolution. To improve the 2θ resolution, we installed a 1-mm-wide block after the sample to reduce the reflected beam width. This blocker rotated with the sample on the goniometer. Figure 2 shows the RSM measurement setup for this low angle incidence GaAs (224).

Figure 3 shows the (004) and (224) RSM data of step-grade (781) and linear-grade (797) samples and the dependence of RSM data (797) on the sample azimuth (ϕ). The substrate peak is the maximum intensity reciprocal lattice point (RLP) at $q_x=0=q_z$ and is used as the reference point for measuring the layer RLP. The three linearly graded samples with dual slopes show results similar to the single slope linear-grade sample. As expected, the step graded

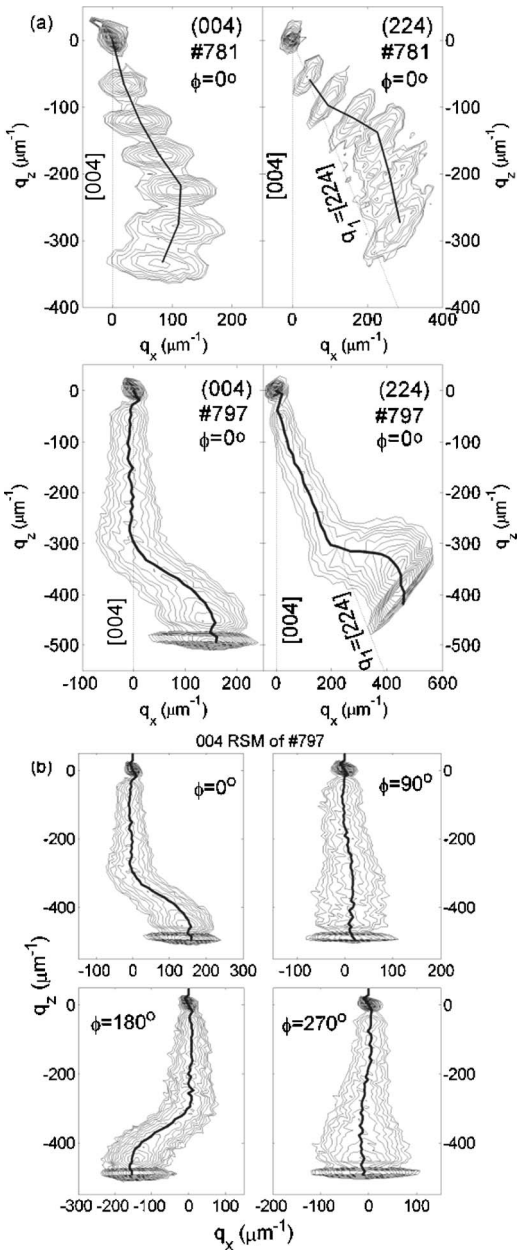

FIG. 3. (a) RSM results of the step-grade (top figures) and a linear-grade (bottom figures) samples. (b) RSM results of a linear-grade sample at four different sample azimuths (ϕ).

buffer shows separable isointensity contours in the RSM, corresponding to each composition layer, and the linearly graded samples show continuously distributed isointensity contour maps along the q_z axis. In the 224 RSM data of Fig. 3(a), the vertical dotted line (marked as [004]) and the inclined dotted line (marked as [224]) indicate the directions along which the RSM intensity will be distributed if the layer was a fully strained epilayer or a completely relaxed epilayer, respectively, assuming that no layer tilt exists. The solid line through the center of RSM contour was obtained by a Gaussian fit to the RSM data at each q_z (for 004 RSM) or q_1 (for 224 RSM) point. The observed deviation of the solid line from the completely strain-relaxed line in the 224 RSM (the inclined line marked as [224]) has two possible contributions: (1) the epilayer is strained and (2) the epilayer is tilted with respect to the substrate. Since the tilt angle influences the RLP peak position, we first removed the tilt contribution. The tilt angle was directly obtained from the 004 RSM data as a function of composition. The depth profile was inferred from it using the fact that the composition varies monotonically for most of the sample depth. The 004 RSM data can be readily used to deduce the layer tilt relative to the substrate because the 004 symmetrical diffraction is only sensitive to the lattice spacing perpendicular to the sample surface. From the 004 RSM, the tilt angle was calculated using the following relation:[16]

$$\text{Tilt angle} = \alpha = \tan^{-1}\left[\frac{|(q_{x,0} - q_{x,180})/2|}{[(4/a_s) - |q_Z|]}\right]. \quad (1)$$

If the epilayer is tilted, the separation of RLPs between the epilayer and the substrate will show a sinusoidal dependence on the sample azimuthal angle according to

$$\alpha = \alpha_0 \cos(\phi - \phi_{\text{ta}}), \quad (2)$$

where α is the measured tilt angle at the sample azimuth ϕ, the azimuthal angle between incident x-ray wave vector and a sample edge $\langle 110\rangle$, and ϕ_{ta} is the tilt azimuth, measured relative to a $\langle 110\rangle$ in-plane direction. The title angle α_0, illustrated in Fig. 4(a), equals the measured tilt angle α only if the tilt axis is parallel to [110] which is normal to the diffraction plane. Therefore, α_0 is obtained by fitting Eq. (2) to the RLP angle separation data obtained from RSM using Eq. (1). Figure 4(a) illustrates these angles and lattice directions. Figure 4(b) shows the tilt angle α_0 thus obtained as a function of q_z, the composition parameter. Table I lists the final values of α_0 and ϕ_{ta} at the sample surface.

Figure 4(b) shows that the tilt angle of the step-grade sample (781) increases with the increasing In composition and decreases slightly at the top, inverse step layer. However, all linear-grade samples show a different tilt characteristic. In the linear-grade samples, the tilt angle is not so significant at low In composition, lower than about In$\approx$60% ($|q_z|$ =310 μm^{-1} for 004 RSM). However, as the In composition increases above 60%, the tilt angle increases abruptly. The tilt angle becomes saturated near the sample surface. This tilt characteristic of the linear-grade samples indicates that two kinds of layer structures are present. This is very interesting and further discussed later in this paper.

Figure 4(c) shows the tilt azimuth data. For the linear-grade samples, the untilted relaxed structure in the lower region was difficult to obtain the tilt azimuth reliably because the low tilt angle means that the lattice planes are nearly parallel to the substrate lattice which in turn makes tilt azimuth data fluctuate wildly. The tilted structure in the upper region of linear-grade metamorphic layer yielded a reliable azimuth data, and this is plotted in Fig. 4(c). The tilt azimuth was somewhere between the $\langle 100\rangle$ and $\langle 110\rangle$ in-plane directions. This is expected from the biaxial nature of mismatch in the interface. This result will be further discussed later in the paper.

The in-plane ($\varepsilon_{\parallel}$) and normal ($\varepsilon_{\perp}$) mismatches were found from the RLP coordinates, q_x and q_z,

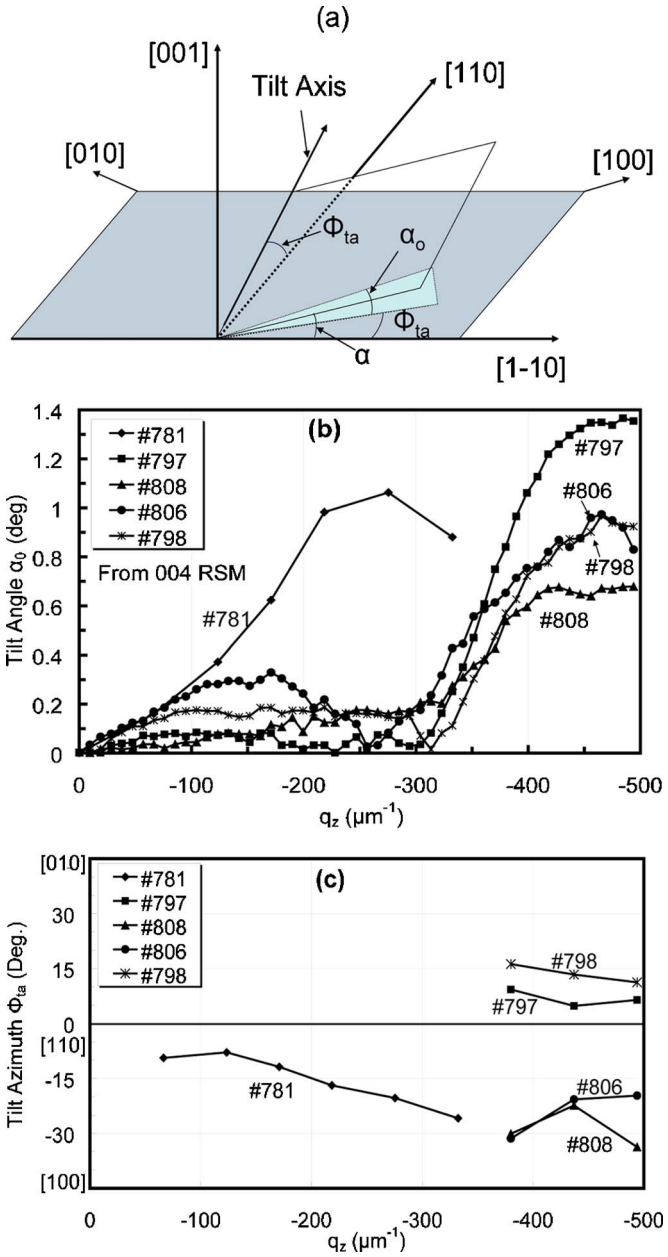

FIG. 4. (a) Definition of tilt angle α_0 and azimuth ϕ_{ta}. (b) Tilt angle α_0 vs q_z, the composition parameter for 004 RSM. (c) Tilt azimuth ϕ_{ta} vs q_z for the step-grade and linear-grade samples. For linear-grade samples, only the upper, tilted regions are plotted.

$$\varepsilon_{\parallel} = \left(\frac{a_{\parallel} - a_s}{a_s}\right)_{0-180,90-270} = -\left(\frac{q_{x,y}}{h_{S,\parallel} + q_{x,y}}\right), \tag{3}$$

$$\varepsilon_{\perp} = \left(\frac{a_{\perp} - a_s}{a_s}\right)_{0-180} = -\left(\frac{q_z}{h_{S,\perp} + q_z}\right). \tag{4}$$

Here, the subscripts of large parentheses indicate the sample azimuth of the 224 RSM data and h_s is the substrate reciprocal lattice vector. The tilt angle correction was done by averaging the RLP positions of sample azimuths that differ by 180°.

Using q_1 position of the RLP as the composition parameter appears to be good for the metamorphic layers as Fig. 5 shows. Here, q_1 is q_{004} or q_z for 004 RSM and q_{224} for 224 RSM. In this figure, the solid line is for a fully strain relaxed layer for which the misfit ε_f and the layer lattice constant a_f are found from

$$\varepsilon_f = \left(\frac{a_f - a_S}{a_S}\right) = \frac{q_1}{h_s}. \tag{5}$$

The data points in Fig. 5 are the measured results from the linearly graded sample 797. The misfit was calculated from the measured RSM data using

$$\varepsilon_f = \left(\frac{a_f - a_S}{a_S}\right) = \left(\frac{1-\nu}{1+\nu}\right)\varepsilon_{\perp} + \frac{\nu}{1+\nu}(\varepsilon_{\parallel,[1\bar{1}0]} + \varepsilon_{\parallel,[110]}), \tag{6}$$

where Eqs. (3) and (4) were used to find the in-plane and normal mismatches, respectively, from the RSM data. The In composition was found from the misfit by applying Vegard's law.

We also obtained, as a function of q_z, the x-ray full width at half maximum (FWHM) along the ⟨110⟩ direction from the 004 RSM data. FWHM was estimated by a Gaussian fitting to the x-ray intensity profile along the ⟨110⟩ direction of the RSM data and averaging over the four sample azimuths ϕ. Figure 6 plots the FWHM data. For linear-grade samples, the x-ray FWHM increases with the increasing In composition until FWHM decreases with increasing In composition above 80%. For the step-grade sample (781), the FWHM increased monotonically with the increasing In composition up to the maximum In content of this sample. Finally, Table I lists the final FWHM and residual strain values at the sample surface.

III. DISCUSSION

For various lattice-mismatched material systems,[2,6,11] the layer tilt is influenced by the unequal distribution of dislocations in the two in-plane directions, such as the two ⟨110⟩ directions for a (001) sample. The layer tilt generally increases as the layer grows thicker for a graded epitaxial layer. The α and β dislocations influence the anisotropy of the residual strain and mismatches in the two in-plane directions and may affect the tilt angle. Other work[6] has suggested that the linearly graded layers have a slower relaxation than the step-graded ones because the strain energy increases more gradually and the tilt angle can be reduced more effectively in a linear grading relative to that in a step grading. Our data show that in the lower In composition regions [$|q_z| < 300\ \mu m^{-1}$ in Fig. 4(b)], the step-grade sample (781) has a much larger tilt than the linear-grade samples. For the linear grade samples and in the high In content region [$|q_z| > 300\ \mu m^{-1}$ in Fig. 4(b)], the layers grown at a slower grading rate (see Fig. 1 for the grading rate) have a larger tilt angle. Our data (Fig. 7) also shows that at the same In composition (i.e., at the same q_1 value in our data), the residual strain is higher in the step-grade sample (781) than in the linear-grade samples. Therefore, our result suggests that a high tilt angle may be concurrent with a high residual strain. A plausible explanation may be that if the material was fully strain relaxed due to a high density of misfit dislocations, for example, then the lattice has little elastic strain and thus no lattice tilting is necessary to accommodate the strain energy.

TABLE I. Summary of x-ray results at the sample surface.

Sample	Buffer	Grading rate	Top layer	Final tilt α_0 (deg)	Final tilt azimuth ϕ_{ta} (deg)	Final FWHM (deg)	Final residual strain
781	Step graded	10% per step six steps	$In_{0.52}Al_{0.48}As$ (480 nm) Inverse step	1.06	−25.86	0.7	-6.9×10^{-3}
797	Linear graded	47% In/μm	InAs (370 nm)	1.35	6.43	0.54	-6.3×10^{-3}
808		$0.05<x<0.15$ 38.5% In/μm $0.15<x<0.95$ 89% In/μm	$In_{0.9}Al_{0.1}As$ (850 nm) Inverse step From InAs	0.64	−22.4	0.9	
806			InAs (1 μm)	0.83	−19.68	1.01	-3×10^{-3}
798		$0.05<x<0.25$ 53.3% In/μm $0.25<x<0.95$ 125% In/μm	InAs (550 nm)	0.92	11.24	0.87	-4×10^{-3}

However, if the material is not fully relaxed and has a significant residual strain, then the lattice needs to tilt itself in order to reduce the elastic strain energy. This view is consistent with the two minimum strain energy structures of lattice-mismatched structures, as discussed in the paper by Dodson *et al.*[13] Elastic strain can be relieved either by misfit dislocations or by lattice tilt. This will be discussed further below. Our data (Figs. 4 and 7) further suggest that the strain relaxation is near complete in the lower regions of the buffer layer for the linear-grade samples, but this is not the case in the step-grade sample.

For a similar grading scheme (e.g., linear grade), a slower grading rate will give more time for the misfit dislocations to glide and for the crystal lattice to adjust by increasing the tilt to accommodate the elastic strains. Our data [Fig. 4(b)] clearly shows that the slowest grading rate sample (797) shows the highest tilt angle near the surface compared to other higher grading rate samples (798, 806, and 808). The slowest grading rate sample (797) also shows the smallest FWHM (see Fig. 6) and the largest residual strain (see Fig. 7) in the near surface region. It is conceivable that a region of the epilayer lies somewhere between an untilted relaxed structure and a tilted structure. For example, when compared with 797 which has a higher tilt angle and lower FWHM, the samples with lower tilt angle and higher FWHM (such as 798, 806, and 808) may have a very small amount of dislocations in the predominantly coherent region.

The tilt angle magnitude suddenly changed as the In composition increased above about 60% (or $q_z=-320$ μm^{-1}) and the tilt angle saturated at its peak value near the In composition corresponding to $q_z=-400--430$ μm^{-1} (see Fig. 4). This is concurrent with the FWHM maximum near $q_z=-380$ μm^{-1} and its subsequent decrease near the sample surface (see Fig. 6). This is also concurrent with the inflection in the residual strain data (Fig. 7) to a steeper rate of increase with the increasing In content at about $|q_1|=500$ μm^{-1} of the 224 RSM (equivalent to $|q_z|=410$ μm^{-1} of 004 RSM). It may be argued that a greater lattice tilt is necessary in order to accommodate a higher elastic strain and less misfit dislocations.

This tilt angle depth profiles of the linear-grade samples are very interesting. The near-substrate region ($|q_z|<320$ μm^{-1}) is an untilted relaxed structure, whereas the

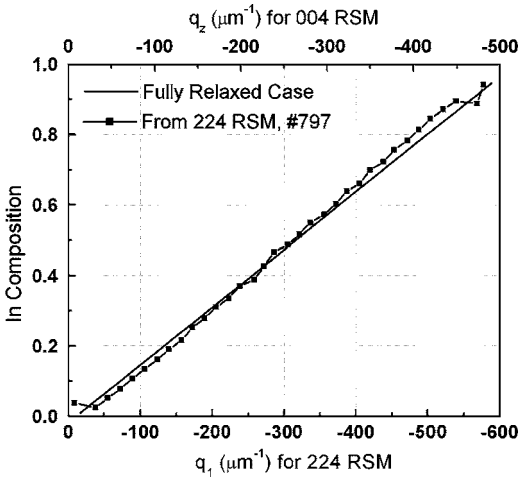

FIG. 5. Indium composition vs the q_1 values of 224 RSM. The solid line is the calculated values for a fully relaxed case. Data points are measured from sample 797. Also shown are the corresponding q_z values for 004 RSM.

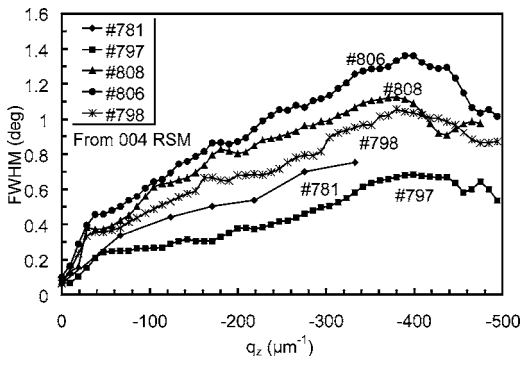

FIG. 6. The x-ray full width at half maximum vs the composition parameter q_z, obtained from 004 RSM data. The x-ray FWHM value is measured along the q_x direction, averaged over the four sample azimuths in Fig. 3(b) as a function of q_z.

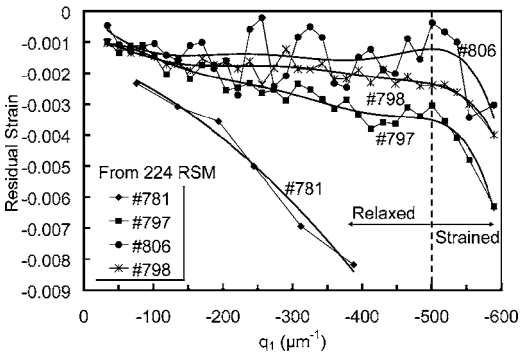

FIG. 7. Residual strain vs q_1 from the 224 RSM data.

upper region ($|q_z|>350\ \mu m^{-1}$) is a tilted structure. Dodson *et al.* have shown that these two structures are the minimum strain energy structures.[13] They argued that the principal driving force for the formation of a tilted interface is the reduction of strain energy of the resulting structure and that the volumetric strain energy is at local minima for a tilted coherent structure and the untilted relaxed structure with an energy barrier separating these two cases. They further argued that for a tilted coherent growth, the effective interplanar mismatch is $\varepsilon(\alpha_0)=\varepsilon_0-a_1(1-\cos\alpha_0)/a_0$, where ε_0 is the lattice mismatch, a_1 and a_0 are the lattice constants for the overlayer and for the substrate, respectively, and α_0 is the tilt angle. Due to this reduced effective mismatch, the tilted structure can grow to a much larger thickness without generating misfit dislocations.

In the linear-grade samples the occurrence of untilted relaxed structure in the lower region and a tilted structure above a certain In composition (about 60% In) presents a distinct possibility for a metamorphic buffer layer design. For example, up to about 60% In where the transition takes place from the untilted relaxed structure to a tilted structure, a higher grading rate may be acceptable. A much slower grading rate may follow for the tilted structure to ensure a high surface quality.

Yamada *et al.*[14] considered a geometrical model to calculate the elastic energy for the tilted coherent growth. For a given number of misfit dislocations over the span of one tilt dislocation (for tilt dislocation, the extra half plane is nearly parallel to the interface), the strain energy minimum occurs at a different tilt angle. They considered either zero or one misfit dislocation per tilt dislocation to be a likely situation. Applying this model to our linear-grade samples and because the overlayer has a larger lattice constant than the substrate, a zero misfit dislocation per tilt dislocation is not a possible option. For one misfit dislocation per tilt dislocation, the approximate tilt angle is 0.7°–1.4° for a lattice mismatch, 1.2%–2.5%. This mismatch is roughly in line with our linearly graded samples if we consider the composition $In_{0.6}Al_{0.4}As$ at the top of the untilted relaxed region to be the "substrate" and the tilted overlayer which ranges linearly from $In_{0.6}Al_{0.4}As$ to InAs in composition to have an average composition of $In_{0.8}Al_{0.2}As$. The mismatch between a coherent $In_{0.8}Al_{0.2}As$ overlayer and the relaxed $In_{0.6}Al_{0.4}As$ substrate is about 1.4%. Therefore, the observed tilt angle of the tilted overlayer, 0.7°–1.4° in Fig. 4(b), is in line with the average mismatch between the tilted overlayer and the underlying relaxed layer.

The residual strain in the linear-grade samples showed a very gradual increase with In content up to 80% ($q_1\approx -500\ \mu m^{-1}$ in Fig. 7) after which it increased more rapidly. The FWHM increases in the plastic relaxation region, $|q_1|<500\ \mu m^{-1}$. This increasing FWHM should be due to the increasing mosaic spread of lattice caused by the high dislocation density in the untilted relaxed layer. The dislocations may contribute to the x-ray FWHM. However, various TEM studies have suggested that the depth profile of dislocation density is approximately uniform.[17,18] The FWHM in the tilted region ($|q_z|>400\ \mu m^{-1}$ in Fig. 6) should be due to the mosaic spread of the lattice due to the underlying relaxed region. TEM images by Chauveau *et al.* also show clearly separable relaxed and coherent regions.[12] Therefore, the FWHM depth profile may be mainly due to the increasing mosaic spread of lattice as the layer grows thicker. The decreasing FWHM toward sample surface suggests that this mosaic spread may be decreasing with the increasing thickness of tilted structure. It should be noted that the 0.6-mm-wide detector slit, used in place of an analyzer crystal, should broaden further the x-ray FWHM of 004 RSM. However, we estimate this additional broadening is small, in the neighborhood of 0.1°, when compared with the experimental FWHM of Fig. 6.

A comparison of the step-grade (781) and linear-grade samples shows that the different growth schemes have a significant effect on the tilt and residual strain. In the linear grade samples, both the tilt angle (Fig. 4) and the residual strain (Fig. 7) are small for low In composition (less than 60% In). However, in the step grade sample (781), in the low In composition region (less than 60%), the tilt angle and the residual strain are high. Transmission electron microscopy (TEM) images of various step-graded III-V compound buffer layers such as InAlAs,[19] InGaAs,[20] and InAsP (Ref. 21) showed that a significantly disordered mosaic structure is present at each interface due to the misfit dislocations. As Fig. 4(b) shows, the tilt angle in the step-grade sample rises rapidly, similar to the linear grade samples of a much higher In content ($|q_z|>310\ \mu m^{-1}$ of 004 RSM). Figure 7 also showed that the residual strain in the step-grade sample with low In content is similar to the strain in the linear-grade samples with a high In content near the sample surface ($|q_1|>500\ \mu m^{-1}$ of 224 RSM). The large tilt angle was concurrent with a large residual strain in the step-grade sample, similar to the linear-grade samples with the high In content of the near-surface region. It is not clear whether the large lattice tilt and the large residual strain, evident in the low In composition region of the step grade sample (781), will persist to a higher In composition (near 100% In) region. It seems still reasonable to conclude that a large lattice tilt and a higher residual strain occur simultaneously regardless of the layer grading scheme. Also, based on our various RSM results (tilt, FWHM, and residual strain), among the samples we studied, the slow grading rate linear grade sample (797) has probably the best surface quality.

It may also be worthy to note that the different linear-

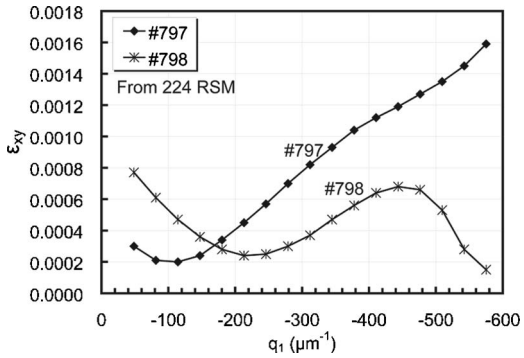

FIG. 8. Shear strain (ε_{xy}) of the linear-grade samples 797 and 798 from 224 RSM.

grading schemes appear to play a role in the tilt and strain characteristics. Above the 60% In composition, after a steep rise in the tilt angle, the single-slope sample (also the slowest grading rate and therefore the thickest) showed the highest tilt angle, largest residual strain, and smallest FWHM near the sample surface. The three dual-slope samples (with a steeper grading rate) showed a relatively smaller tilt angle, smaller residual strain, and larger FWHM at the surface than the single slope sample. However, the effect of different linear grading schemes is probably only secondary to the effects of the grading rate in determining the structural quality of the surface.

For the step-grade sample (781), the tilt azimuth ranged from 9° away from ⟨110⟩ in the low In composition region to 26° from ⟨110⟩ in the top $In_{0.6}Al_{0.4}As$ layer. The tilted region of the linear-grade samples has a tilt azimuth between 5° and 35° away from ⟨110⟩ with a general tendency of having a smaller deviation of azimuth from ⟨110⟩ for a higher tilt angle (797) and a larger deviation for a smaller tilt angle (808). This observation appears to suggest that a best quality (i.e., lowest FWHM such as 797) linear-grade layer has its tilt axis closely aligned with ⟨110⟩, whereas the linear-grade samples with a higher FWHM and a lower tilt angle (such as 806 or 808) have their tilt azimuths deviating farther away from ⟨110⟩ and closer to ⟨100⟩. Table I summarizes the above results for each sample. It lists the values in the maximum In composition region for tilt angle α_0, tilt azimuth ϕ_{ta}, FWHM, and residual strain.

Finally, it should be noted that the lattice tilt is related to the different amounts of relaxations along the two ⟨110⟩ in-plane directions. In Fig. 4(b), in the near-surface region ($|q_z| > 320\ \mu m^{-1}$), the single-slope sample (797) showed a higher tilt angle than the steeper-grade samples. From this result, one may argue that the single slope sample (797) has a higher anisotropic strain relaxation. This nonequal relaxation along the two ⟨110⟩ directions is the elastic shear strain[22] $\varepsilon_{xy} = \psi = \varepsilon_{[110]} - \varepsilon_{[1-10]}$. Figure 8 shows the shear strain variation of the two linearly graded samples, 797 and 798. In the near-surface region ($|q_1| > 450\ \mu m^{-1}$ in Fig. 8), sample 797 had a higher shear strain than sample 798, and the tilt angle data in Fig. 4(b) showed that 797 had a higher tilt angle.

IV. SUMMARY

The structural properties of metamorphic $In_xAl_{1-x}As$ ($0.05 < x < 1$) buffer layers grown on GaAs substrates were investigated using the high resolution x-ray reciprocal space mapping technique. Although the RSM measurements were used before in studying the metamorphic buffer layer samples, this paper extended the RSM analysis to the depth-dependent strain relaxation, tilt angle and tilt azimuth, and the x-ray FWHM of metamorphic samples. Several reciprocal space maps were measured at a different azimuthal angle. Three types of metamorphic samples were examined in this work, including step-graded, single-slope linearly graded, and dual-slope linearly graded buffer layer samples. All buffer layers showed a net tilt angle with respect to the substrate. The tilt angle variation was different for the linear grade samples from the step grade sample. The linearly graded samples had very low tilt angle for In composition below 60%. Above this In composition, the tilt angle increased abruptly. In contrast, the tilt angles in the step-graded sample increased gradually starting at the substrate-buffer interface. Tilt axis lied somewhere between ⟨110⟩ and ⟨100⟩ in-plane directions. The tilt azimuth had a general tendency of being closer to ⟨110⟩ for higher tilt angle and higher quality (lower FWHM) sample (797) and closer to ⟨100⟩ for lower tilt angle and lower quality (higher FWHM) sample (808, for example). Of particular interest was the fact that both of the minimum strain energy structures occurred in all linear-grade samples: the untilted, fully relaxed layer (the plastic relaxation region near the substrate), and the tilted layer (elastic region near the surface), which have been discussed in the work by Dodson *et al.*[13] [see Fig. 4(b)]. Furthermore, the tilt angle of the top region was in reasonable agreement with the minimum elastic energy model by Yamada *et al.*[14] It may be argued therefore that the growth strategy of a metamorphic buffer layer (that is, minimizing the growth time while maximizing the surface quality) may be achieved by a fast grading rate for the untilted relaxed region (up to $In_{0.6}Al_{0.4}As$ in our samples) and a slow growth rate of the tilted structure for the best surface quality.

[1] W. E. Hoke *et al.*, J. Cryst. Growth **251**, 804 (2003).
[2] H. Ehsani, I. Bhat, R. J. Gutmann, G. Charache, and M. Freeman, J. Appl. Phys. **86**, 835 (1999).
[3] M. Sexl, G. Bohm, M. Maier, G. Trankle, G. Weimann, and G. Abstreiter, Compound Semicond. **156**, 49 (1998).
[4] A. Bosacchi *et al.*, J. Cryst. Growth **175**, 1009 (1997).
[5] J. C. P. Chang, J. H. Chen, J. M. Fernandez, H. H. Wieder, and K. L. Kavanagh, Appl. Phys. Lett. **60**, 1129 (1992).
[6] J. I. Chyi, J. L. Shieh, J. W. Pan, and R. M. Lin, J. Appl. Phys. **79**, 8367 (1996).
[7] K. L. Kavanagh, J. C. P. Chang, J. Chen, J. M. Fernandez, and H. H. Wieder, J. Vac. Sci. Technol. B **10**, 1820 (1992).
[8] J. A. Olsen, E. L. Hu, S. R. Lee, I. J. Fritz, A. J. Howard, B. E. Hammons, and J. Y. Tsao, J. Appl. Phys. **79**, 3578 (1996).
[9] M. Haupt, K. Kohler, P. Ganser, S. Muller, and W. Rothemund, J. Cryst. Growth **175**, 1028 (1997).
[10] E. Towe, D. Sun, and B. R. Bennett, J. Vac. Sci. Technol. B **12**, 1099 (1994).
[11] J. H. Li, V. Holy, G. Bauer, J. F. Nutzel, and G. Abstreiter, Semicond. Sci. Technol. **10**, 1621 (1995).
[12] J. M. Chauveau, Y. Cordier, H. J. Kim, D. Ferre, Y. Androussi, and J. Di Persio, J. Cryst. Growth **251**, 112 (2003).

[13]B. W. Dodson, D. R. Myers, A. K. Datye, V. S. Kaushik, D. L. Kendall, and B. Martinez-Tovar, Phys. Rev. Lett. **61**, 2681 (1988).
[14]A. Yamada, P. J. Fons, R. Hunger, K. Iwata, K. Matsubara, and S. Niki, Appl. Phys. Lett. **79**, 608 (2001).
[15]R. Du and C. P. Flynn, J. Phys.: Condens. Matter **2**, 1335 (1990).
[16]J. M. Chauveau, Y. Androussi, A. Lefebvre, J. Di Persio, and Y. Cordier, J. Appl. Phys. **93**, 4219 (2003).
[17]S. I. Molina, F. J. Pacheco, D. Araujo, R. Garcia, A. Sacedon, E. Calleja, Z. Yang, and P. Kidd, Appl. Phys. Lett. **65**, 2460 (1994).
[18]F. Romanato *et al.*, J. Appl. Phys. **86**, 4748 (1999).
[19]C. Heyn, S. Mendach, S. Lohr, S. Beyer, S. Schnull, and W. Hansen, J. Cryst. Growth **251**, 832 (2003).
[20]P. Kidd *et al.*, J. Cryst. Growth **169**, 649 (1996).
[21]M. K. Hudait, Y. Lin, D. M. Wilt, J. S. Speck, C. A. Tivarus, E. R. Heller, J. P. Pelz, and S. A. Ringel, Appl. Phys. Lett. **82**, 3212 (2003).
[22]C. R. Wie, Mater. Sci. Eng., R. **13**, 1 (1994).